Dependence of *J*-integral and Failure Assessment Diagram on Strength Mismatching and Crack Length for Welded Joint Specimen†

Hidekazu MURAKAWA*, Yongping LEI, Yaowu SHI*** and Yukio UEDA******

Abstract

In this paper five kinds of strength matching weldments are considered. The degree of matching is defined by the match factor M, a ratio of yield strength of weld metal to that of parent metal. The values of M are chosen to be 1.4, 1.2, 1.0, 0.8 and 0.6, respectively. Five typical ratios of half crack length to half specimens width from shallow to deep: a/W = 0.1, 0.175, 0.25, 0.375 and 0.5 are assumed. Center-cracked panel (CCP) specimens with weld joints are numerically analyzed by using the elastic-plastic finite element method. The emphasis is placed on the effects of the strength matching factor and the crack length on the J-integral as well as the shape of the failure assessment curve (FAC). The most complex option, termed as option 3 in the third revision of R6, is used to generate the FAC. It is demonstrated that the strength mismatching of a welded joint has a great influence on the value of the J-integral and the shape of FAC, but the influence of crack length is relatively small. The increase of M for cases the with same value of a/W expands the safe region in the failure assessment diagram (FAD), and conversely a decrease of M makes it contract. From the numerical results, it is concluded that when making a failure assessment for the initiation of fracture from defects in a welded structure, the FAC obtained by using the finite element method under the conditions of real mismatched joints should be adopted. However, when option 1 or option 2 are selected, the engineering formulae of these two options should be revised in consideration of the influence of strength mismatching of welded structures.

KEY WORDS: (Fracture) (Strength Mis-Matching) (Failure Assessment) (*J*-Integral) (Finite Element Method)

1. Introduction

Many important structures such as pressure vessels, pipelines and offshore structures are assembled by welding. Due to the choice of the weld metal and the local thermal cycle, the region near the weld joint becomes heterogeneous in mechanical properties. Also, flaws or cracks are often produced in the welded joints during welding process and/or in service. Therefore, the prediction of the defects initiating crack growth is of great importance for proper assessment of the overall strength of these structures. For the above reasons, in recent years, considerable efforts have been devoted to establishing heterogeneous elastic-plastic fracture mechanics[1-6]. Many of them have paid attention to the influence of nonhomogeniety in material properties and residual stress due to welding on various fracture parameters[4-6]. However, relatively few studies have been made on the effect of the strength mismatching on the failure assessment diagram.

At the same time, many methods have been developed to assess the integrity of structure containing defects, such as the crack-tip opening displacement design curve approach, the *J*-integral based on the methods of EPRI (Electric Power Research Institute/General Electric) and CEGB/R/H/R6(Central Electricity Generating Board) failure assessment procedures. In the R6 method, three options are given for describing the failure assessment curve, and these are described in detail in the references of Milne[7]. It has been extensively validated that the procedures of R6 are suitable for assessing cracked structures with homogeneous materials[8,9]. For welded structures, or their components, the ability of the method

† Received on May 19, 1997
* Associate Professor
** Associate Professor, Xi'an Jiaotong University
*** Professor, Beijing Polytechnic University
**** Professor, Kinki University
Transactions of JWRI is published by Joining and Welding Reseach Institute of Osaka University, Ibaraki, Osaka 567, Japan.

to provide accurate and safe defect assessment is uncertain because of the inherent mechanical and metallurgical heterogeneity of the weldment.

The purpose of the present work is to examine the effects of a strength mismatching factor M (yield strength of weld metal/yield strength of parent metal) and crack length on the value of J-integral (crack driving force) as well as the shape and position of FAC (Failure Assessment Curve) for welded joint specimens. The finite element results for center-crack panel (CCP) specimens subjected to tension are presented. A commercial finite element program ABAQUS is used. This work provides a fundamental basis for evaluating the crack driving force and FAD (Failure Assessment Diagram) of welded joint specimens with different strength matching factor and crack length.

2. Basis of R6 Procedures

The assessment of defects in flawed structures by the R6 failure assessment method is based on the plastic collapse load of the structure, and the stability of the defect under linear-elastic fracture mechanics criterion. Therefore, to make the integrity assessment for structure containing defects using the R6 procedures, two parameters must be calculated for the component containing a defect of size, a, and a applied load, P. These parameters are denoted as K_r and L_r in the notation of R6 and are defined by[7,9]

$$K_r = \frac{K_1(P,a)}{K_{1c}} \tag{1}$$

$$L_r = \frac{P}{P_0(a,\sigma_y)} \tag{2}$$

where K_1 is the linear elastic stress intensity factor, K_{1c} is the fracture toughness, σ_y is the yield stress and P_0 is the value of P corresponding to plastic yield load of the flawed structure. Having evaluated K_r and L_r, the integrity can be judged through the relative position of the point (L_r, K_r) within the FAD. The failure by fracture from the defect is avoided if the point lies within the safe area bounded by a failure assessment curve and the axes. Otherwise, the structure is unsafe.

The failure assessment diagram constructed in R6 is based on two criteria. The first is avoidance of fracture under linear elastic conditions and the second is avoidance of failure by plastic collapse. These two limits in R6 are represented by

$$K_r \le 1 \tag{3}$$

$$L_r \le L_r^{\max} \tag{4}$$

where $L_r^{\max}$ is defined in terms of the uniaxial flow stress, $\overline{\sigma}$, and yield stress, σ_y by

$$L_r^{\max} = \frac{\overline{\sigma}}{\sigma_y} \tag{5}$$

The criteria of inequalities (3) and (4) only define two limits in the FAD. The intermediate elastic-plastic region is included in R6 by replacing inequality (4) with

$$K_r \le f(L_r) \tag{6}$$

When parameter J-integral is used, the failure assessment curve, $f(L_r)$, has the form as follows

$$f_3(L_r) = \left(\frac{J}{J_e}\right)^{-1/2} \tag{7}$$

This definition is based on the equivalence of the failure assessment curve to J-integral analysis. The relevant FAD is termed as option 3 in R6 and is noted by the subscript 3 in Eq.(7). J and J_e are the values of J-integral obtained from an elastic-plastic analysis and elastic analysis respectively for the same load. This curve is dependent on both material and geometry.

For the option 2 curve of R6, the FAC related to elastic-plastic fracture is described by the equation

$$f_2(L_r) = \left\{\frac{E\varepsilon_{\text{ref}}}{L_r\sigma_y} + \frac{L_r^3\sigma_y}{2E\varepsilon_{\text{ref}}}\right\}^{-1/2} \tag{8}$$

where $\sigma_{\text{ref}} = L_r\sigma_y$ and ε_{ref} is the true strain obtained from the uniaxial stress/strain data at a true stress level σ_{ref}. E is Young's modulus. The main features of option 2 are that the diagram depends only on material stress/strain response, so it is suitable for all metals regardless of their stress-strain behaviors.

For the option 1 curve of R6, the FAD related to elastic-plastic fracture is described by the following equation

$$f_1(L_r) = [1 - 0.14L_r^2][0.3 + 0.7\exp(-0.65L_r^6)] \tag{9}$$

Equation (9) is obtained by empirically fitting to option 2 curves for a variety of materials, but biased towards the lower bound. With this option, only the yield and ultimate tensile stresses are needed to define the upper limit, $L_r^{\max}$ of Eq.(5) rather than details of stress-strain data. Thus, the curve is independent of both material and geometry .

The above descriptions of the three options of failure assessment curve in the R6 procedure provide three levels of analysis. Because the option 3 curve of Eq.(7) is derived from J-integral value, either computed by finite-element analysis or measured by experiment, it has greater potential in terms of accuracy than the approximate curves of option 1 and 2. Therefore, all the present calculation for the failure assessment curves are based on the option 3, but the failure assessment curves of option 1 and 2 for parent metal (even-matching) are also computed for comparison.

3. Numerical Model and Computational Procedures

When steel plates are welded by submerged arc welding, the mechanical properties are generally different among the parent metal, the heat affected zone (HAZ) and the weld metal. On the other hand, when a filler material with different levels is used, or when the different welding processes or different joint type are selected, different strength matching of weld metal can be obtained for the same parent metal. In the present work, the welded joint is modeled to consist of two materials, namely the weld metal and parent metal. The presence of any HAZ or transition region between the two materials is ignored in all of the computations. To consider the difference of strength mismatching, two undermatching weld metals (M=0.8 and 0.6), two overmatching weld metals (M=1.2 and 1.4) and evenmatching weld metal (M=1) are selected. In the computation of each specimen, the weld metal and parent metal themselves are treated as homogeneous in mechanical properties. Only the strength of the weld metal is changed for different specimens according to the strength matching factor M. The parent metal is a nuclear pressure vessel steel A508C13, and its mechanical properties are given in **Table 1**[10]. Based on these properties of parent metal, the welded joints with different strength matching factor are determined and are summarized in **Table 2**. The strain hardening exponent of the weld metal is calculated according to the following empirical formula[11]

$$n = \frac{1}{0.1627 \cdot \ln(1390/\sigma_y)} \tag{10}$$

It should be mentioned that the constant 0.1627 in Eq.(10) is a value recalibrated by using the experimental properties of the A508C13 and is different from the value given in the reference.

Table 1 Mechanical properties of A508C13.

σ_y (MPa)	σ_{UTS} (MPa)	δ_5 (%)	Φ (%)	n*
540	642	22	73	6.5

* n— Strain hardening exponent

Because the failure assessment curve evaluated using option 3 in R6 depends on both material stress/strain behaviors and on geometry, the following power law constitutive equation is used in the present computation for both weld metal and parent metal:

Table 2 Material properties of welded joint for computation.

	Weld metal				Parent metal	
	σ_y (MPa)	n	σ_y (MPa)	n	σ_y (MPa)	n
Undermatch	648	8.05	756	10.09	540	6.5
Evenmatch	540	6.5	540	6.5	540	6.5
Overmatch	432	5.26	324	4.22	540	6.5

$$\text{if } \sigma \le \sigma_y: \ \varepsilon = \frac{\sigma}{E}$$
$$\text{if } \sigma \ge \sigma_y: \ \varepsilon = \varepsilon_y \left\{ \alpha \frac{\sigma}{\sigma_y} \right\}^n \tag{11}$$

The above stress-strain relations are plotted in **Fig.1**. These data are perhaps somewhat different from the value of weld metal in real situation, but the results of computation would still provide meaningful information about the influence of strength mismatching. Young's modulus (E) and Poisson's ratio are equal to 210 (GPa) and 0.3, respectively.

The specimens are modeled as two dimensional center cracked panels (CCP). The specimen size is 160×80 mm and the width of weld metal is 20 mm, as shown in **Fig.2** by the hatched area. The half crack length is selected as 4, 7, 10, 15 and 20 mm to cover the situation from shallow crack to deep crack. The values of a/W (crack length/specimen width) corresponding to those crack length are 0.1, 0.175, 0.25, 0.375 and 0.5, respectively.

In the present analyses, the cracks are assumed to be stationary, and considering that the vessel diameter is far larger than the wall thickness in most real situations, the plane stress state is assumed for all of the computations. The numerical computations are carried out using the

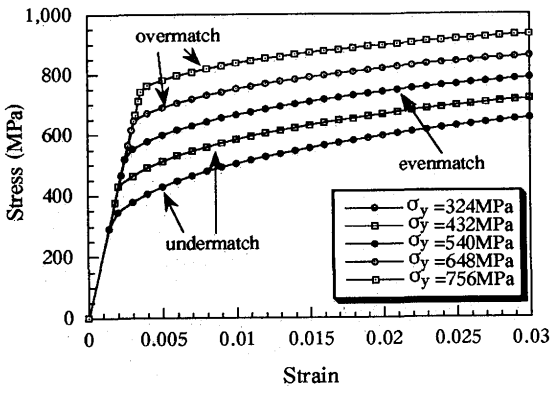

Fig.1 Stress and strain relations of the parent metal and different strength mismatching weld metals

finite element code ABAQUS[12]. An eight-node isoparametric element CPS8 in the ABAQUS element library is used for elastic and elastic-plastic analyses. The crack tip is modelled using stress singularity elements. Incremental plasticity and von Mises yield criteria with the associated flow rule are adopted. The load is applied to 1.5 times the limit load through load-controlled loading. The load increments up to the maximum load are 200 steps.

Due to the symmetry, only one fourth of the specimen is considered. The finite element mesh for a/W=0.25 is shown in **Fig.3**, in which a total of 336 elements and 1095 nodes are incorporated. The base mesh configurations for other crack lengths are the same as a/W=0.25, but the numbers of mesh and nodes may be different.

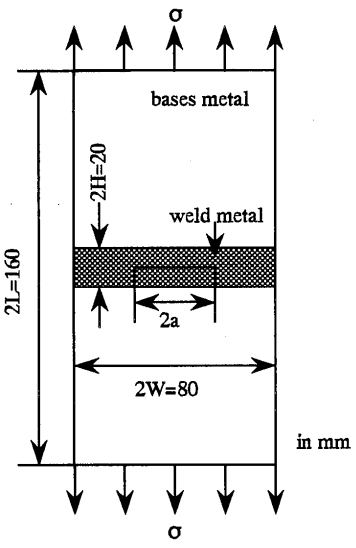

Fig.2 Schematic illustration of the computational model, center cracked panel specimen containing transverse mismatched weld.

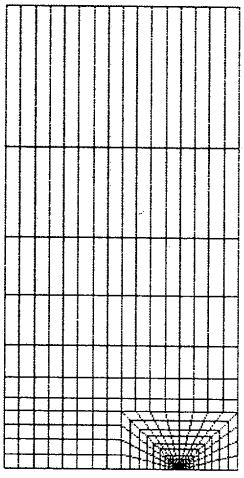

Fig. 3 Typical computational mesh for one fourth of the specimen.

4 Results and discussions

4.1 Effect of weld strength mismatching and crack length on J-integral values

Since the failure assessment diagrams have been plotted according to the options of the third revision of R6 in the present studies, it is necessary to know the plastic yield load P_0 of the specimens to evaluate the load parameter L_r in Eq.(2). For plane stress condition, it is given by

$$P_0 = \sigma_y(2W - 2a) \tag{12}$$

where σ_y is the yield stress of the material, W is the half width of specimen, a is the half width of the crack.

Because J-integral is an important parameter in determining the fracture characteristics of the specimen, also the option 3 in R6 is based directly on the equivalence of FAC to J-integral, the relation of J-integral with applied load, which is normalized by plastic yield load, P_0 , is generated by the finite element analysis during the loading process.

Figure 4 shows the effects of the strength mismatching in welded joints on the relations of J-integral *vs.* loading for the selected five different a/W. It can be seen that the strength matching factor M has a great influence on the J-integral. For each strength matching factor M, the J-integral values are increased with increasing normalized load P/P_0. However, their increasing rates are different. For undermatched joint specimens, the J-integral values are greater than those of the evenmatched joint specimens when they have the same applied load. This tendency becomes clear when P/P_0 is greater than 1.0. On the other hand, for overmatched joint specimens, the situations are just the opposite. These effects of the strength matching factor M on the J-integral are the same for the specimens with different crack lengths.

To indicate clearly the influence of strength matching factor M on the J-integral value, Fig.4 has been replotted into **Fig.5**. It can be seen from Fig.5 that the J-integral value increases with decreasing strength matching factor M for each normalized load P/P_0, especially when P/P_0 is greater than about one. At this point the yielding region ahead of the crack tip may be changed from small-scale to large-scale or fully yielding. That means for the same parent metal, the J-integral crack driving forces of the overmatched joint specimen are always smaller than those of the undermatched joint specimens under the condition of the same P/P_0 and a/W. It may be inferred that the fracture-resistance capability of overmatched welded joints is larger than those of undermatched welded joints. This result is quite similar to the previous investigation on the three-point bend specimens[13],

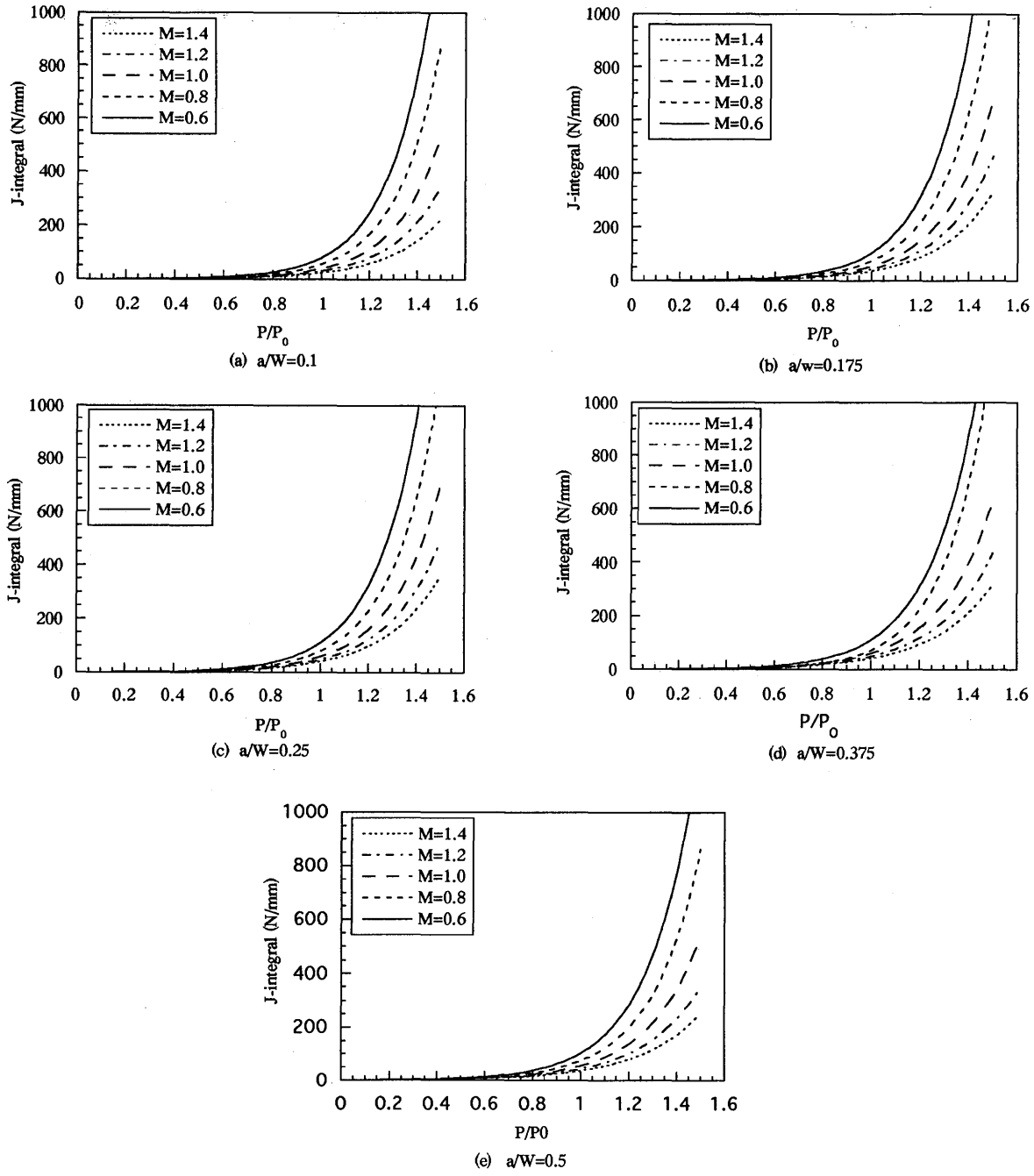

Fig.4 Effect of welded joint strength matching factor M on the relation of *J*-integral and normalized load.

and can be explained by the occurrence and development of the plastic deformation region ahead of the crack tip. In case of the undermatched welded joint specimen, the deformation is mainly confined within the weld metal during the loading process because the weld metal strength is relatively lower compared with the parent metal. On the contrary, when the joint is overmatched, the plastic zone spreads beyond the weld boundary and extends into the parent metal, thus deformation can be promoted by the yielded parent metal, and the concentrated stress at the crack tip is partly relaxed when the specimens have the same crack depth and normalized loading. This is the reason why overmatched welded joints possess a higher fracture-resistant capacity than the undermatched welded joints for the same crack length.

In order to investigate the effect of crack length on the *J*-integral crack driving force, **Figure 6** is replotted from Fig.4, in which a/W is chosen as a variable on the

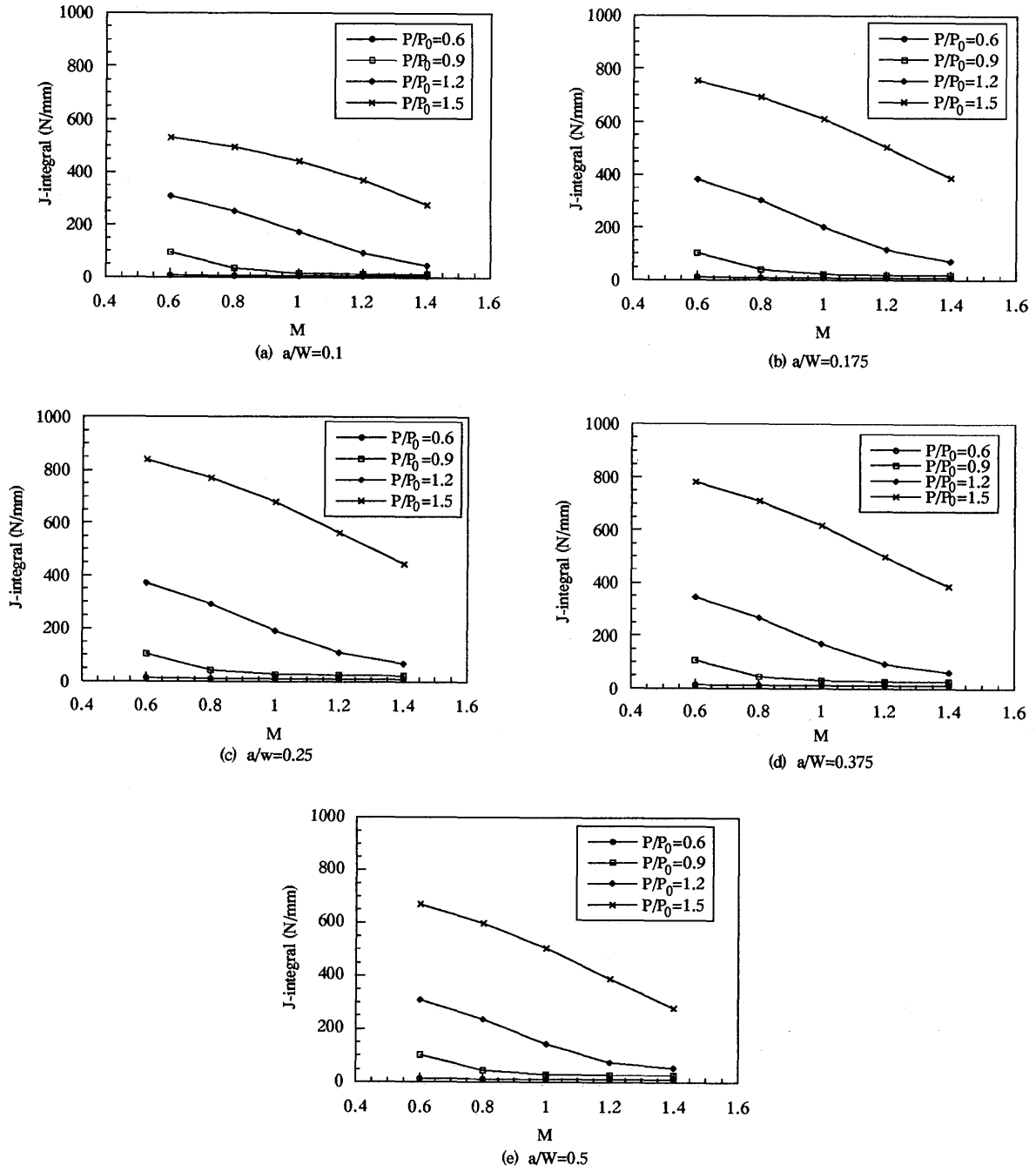

Fig.5 Effect of normalized load on the relation of J-integral and strength matching factor M.

abscissa. It is indicated that when P/P_0 is less than 1.0, the crack length only gives a small influence on the J-integral, although the values of J-integral are different for the specimens with different strength matching factor. However, it can be seen that the J-integral values have a very small difference among different crack depths when the curves corresponding to P/P_0=0.9 are compared. The values for long cracks are slightly higher than those for short cracks. When P/P_0 is greater than one, the influence of crack length on the J-integral gradually becomes notable. With an increase of a/W, the J-integral value first increases, and then reaches a peak value, thereafter decreases. Moreover, the position corresponding to peak value is different for different P/P_0. For instance, when P/P_0=1.2, a/W corresponding to the peak J-integral is 0.175 and when P/P_0=1.5, a/W corresponding to the peak is 0.25. This tendency is the same for the specimen with different strength matching

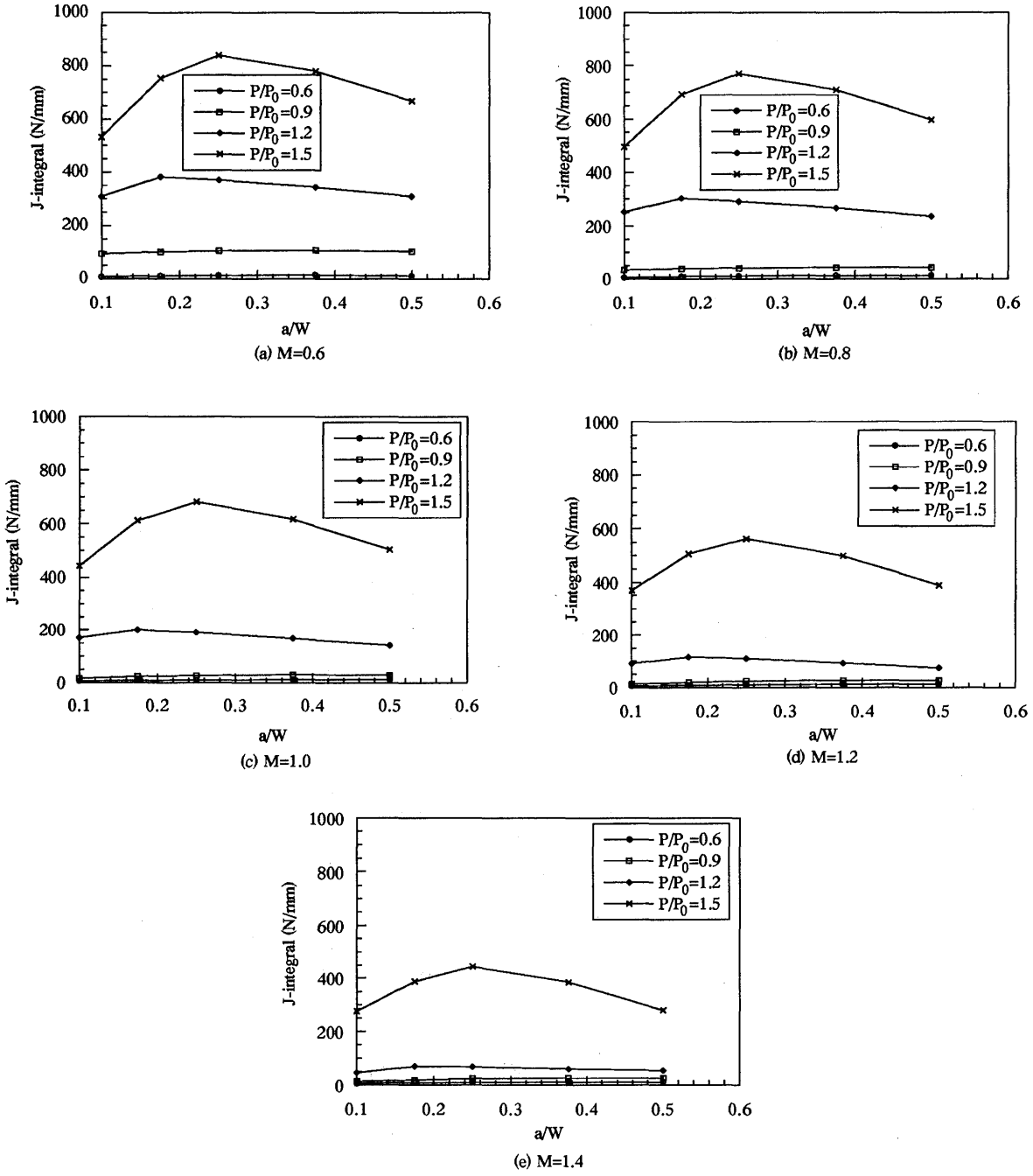

Fig.6 Effect of normalized load on the relation of J-integral and crack length.

factors M. This relation between the J-integral and the crack length may be explained by the test results reported by the authors[14]. It has been indicated that there exists a peak in the J-integral curve for the onset of crack growth when the specimens have the crack size a/W from 0.005 to 0.5.

4.2 Effect of strength mismatching and crack length on the failure assessment curve

The failure assessment diagrams are computed for the selected five typical strength matching factors M and five typical ratios of crack length to specimen width using Eq.(7) for the material properties given by Table 2. The material constitutive relation of stress and strain are computed by Eq.(11). **Figure 7** shows the dependence of failure curves on the strength matching factors for different a/W. In order to make a comparison, the failure assessment curves of evenmatched welded joint specimens

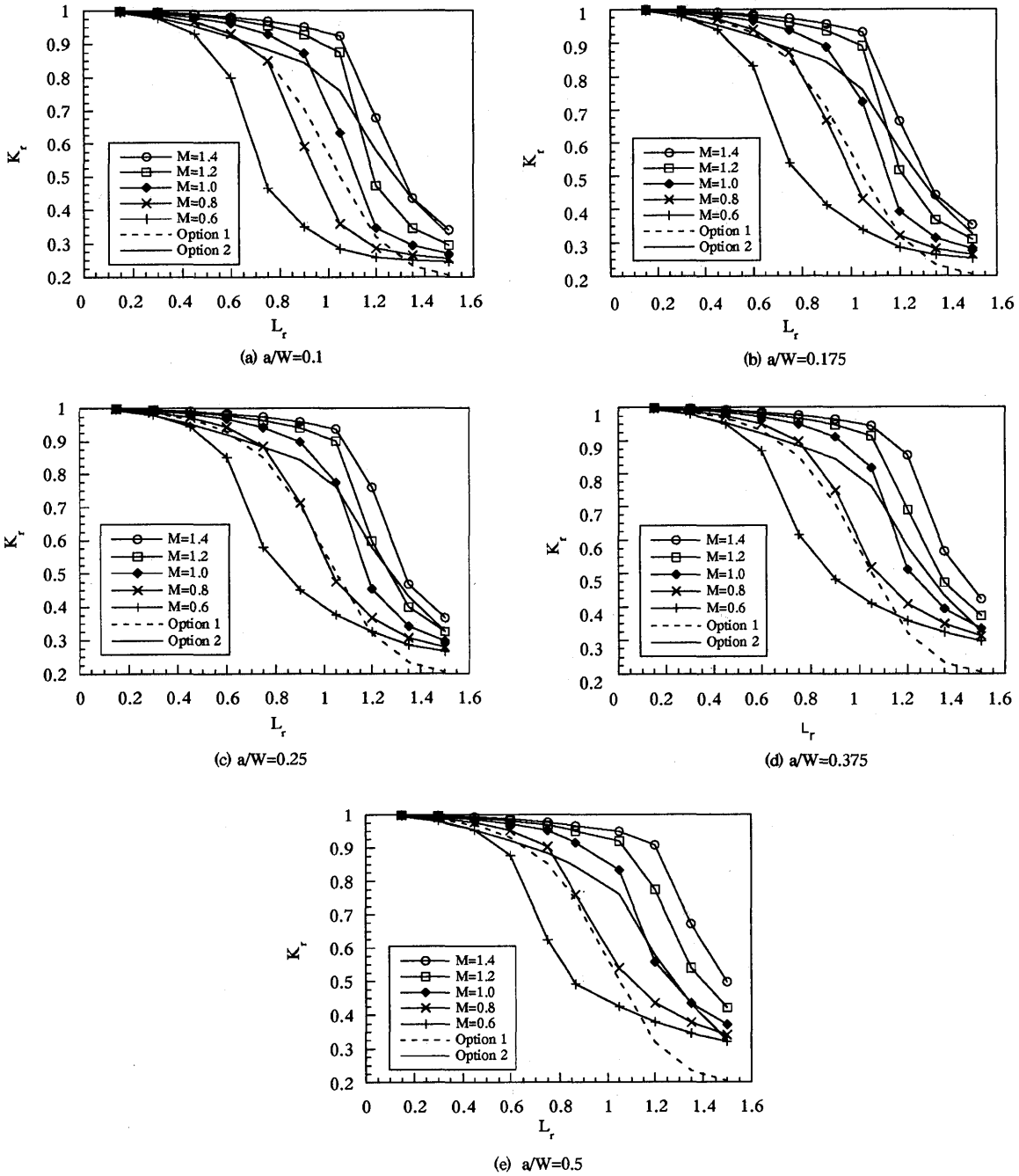

Fig.7 Failure assessment diagram of center-cracked specimens ---dependence of failure curves on the welded joint strength matching factor M for different crack lengths.

computed by Eq.(9) (option 1) and Eq.(8) (option 2) are also plotted in Fig.7 in which they are indicated by dashed line and solid line, respectively. It is apparent for each value of a/W that the failure curves are dependent on the strength matching factors. The curves for overmatched joint specimens always lie over the curve of evenmatched joints. On the contrary, the curves of undermatched joint specimens always locate below those of the evenmatched joint specimens. For overmatched welded joints, the greater the strength matching factor is, the higher the failure curve locates. For undermatched joints, the smaller the strength matching factor is, the lower the failure curves locates. This means that for the same a/W the safe region bounded by the axes and the failure curve becomes wider when a welded joint is overmatched, while the safe region is small for a undermatched weld joint. It can be also seen from Fig.7 that the curve for option 1 is not conservative when the

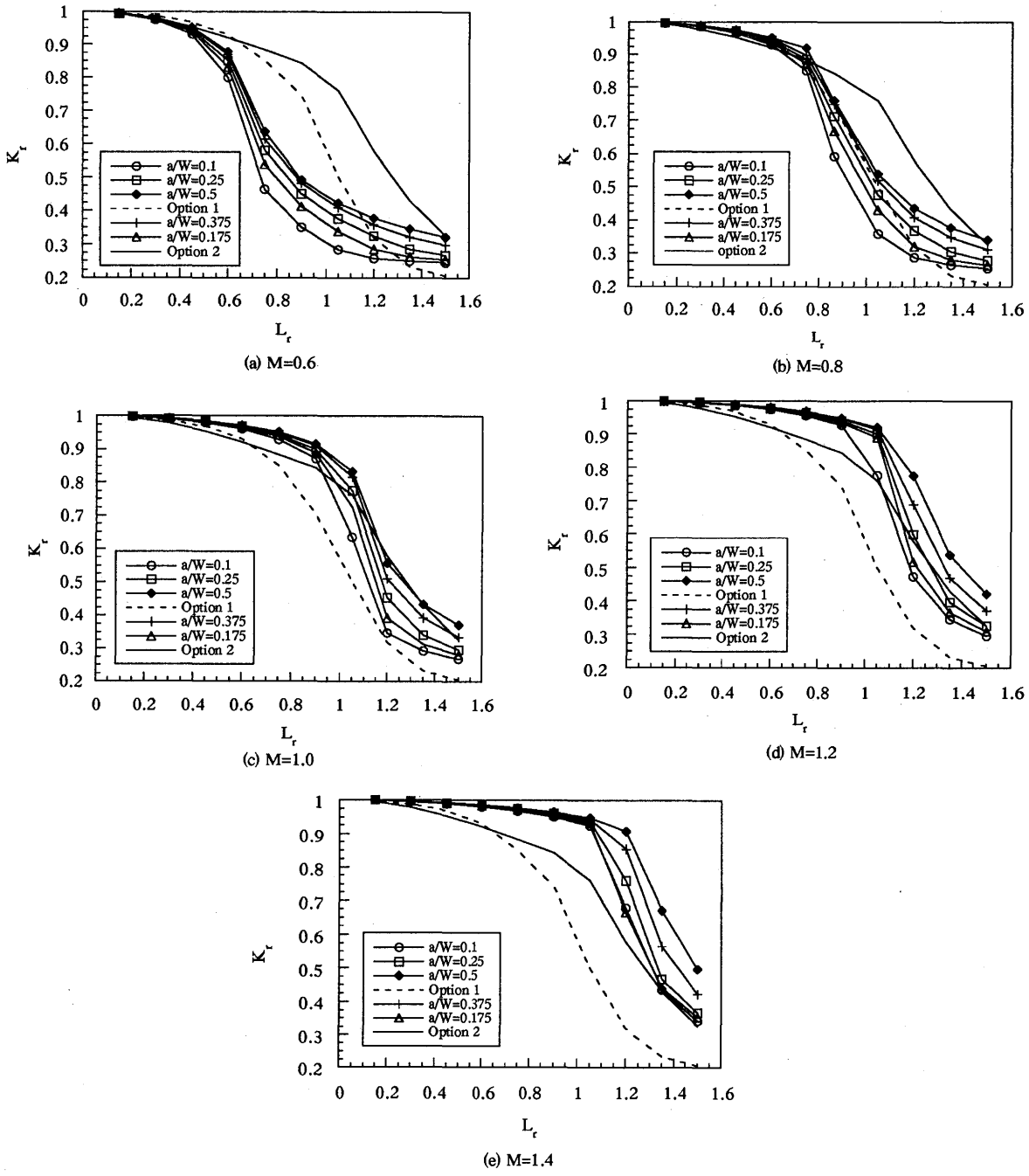

Fig.8 Failure assessment diagram of center-cracked specimens ---dependence of failure curves on crack length for different welded joint strength matching factors M.

strength matching factor is less than 0.8, even though it is a fitted curve to that of the option 2 for a variety of materials and biased towards the lower bound. That is to say, the option 1 failure assessment curve is only suitable for the overmatched and evenmatched weld joints or undermatched joints when the strength matching factor is greater than 0.8. The reason may be that when establishing Eq.(8) (option 2) the effect of strength mismatching factor is not considered.

The predicted results clearly revealed that the shape and position of the failure curve in the diagram with respect to K_r and L_r are significantly influenced by the strength matching factor. Thus, Eqs. (9) and (8) corresponding to option 1 and option 2 of R6 should be revised in consideration of the influence of the strength mismatching of the welded structures.

The influence of the relative size of the crack a/W on the failure curves is given in **Fig.8** for different strength

matching factors. Compared with Fig.7, the failure curves show slight dependence on a/W. For different a/W and with the same M, the curves are close to each other. Those lines with greater a/W locate slightly over those with smaller a/W. In view of Fig.8(a) to Fig.8(e), it can be also seen that the safe region is extended with an increase of strength matching factor M.

5. Conclusion

To explore the influence of the strength mismatching factor at the weld joint and crack length as well as their interaction on the J-integral as crack driving force and the failure assessment curves described in terms of K_r and L_r, a series of numerical calculation on CCP weld joint specimen were performed by using FEM. The following results were obtained:

1) In view of the overall predicted results, the J-integral crack driving force and the shape and position of failure assessment curves are strongly affected by strength mismatching when the crack length to width ratio a/W is between 0.1 and 0.5. With an increase in strength matching factor M, the J-integral at the higher loading ($P/P_0 \geq 0.9$) is decreased, and the area of the safe region in FAD is extended.
2) When $P/P_0 < 1.0$, the crack lengths have small influence on the J-integral. The J-integral for a long crack is slightly higher than that for a short crack. However, when $P/P_0 \geq 1.0$, this influence becomes notable. With the increase of a/W, the J-integral first increases, and then decreases after reaching a peak value. For different P/P_0 the positions corresponding to the peak value are different. This tendency is the same for the specimen with different strength matching factors.
3) The failure assessment curves of overmatched weld joint specimens are always in the higher position compared to the evenmatched joints. On the contrary, the curves of undermatched weld joint specimens are always lies below those for the evenmatched joints.
4) When the strength matching factor M is less than 0.8, the option 1 curve of R6 can not give a conservative result.
5) Compared with the strength matching factor, the effect of crack length on the shape and position of the failure curve is relatively small. The failure curves with greater a/W are slightly higher than those with smaller a/W.
6) When making an assessment for the initiation of fracture from defects in welded structure, an FAD obtained by using a finite element method considering real mismatching should be employed. However, when the option 1 or option 2 of R6 are selected, the engineering formulae of these two options should be revised in consideration of the influence of strength mismatching of weldment.

References

1) S.Aoki, N.Ishii and X.F.Luo, 3-D elastic-plastic finite element analysis of interface cracks under mixed mode load, *Engineering Fracture Mechanics*, Vol.63, pp.327-338, 1996
2) T.Nishioka, Y. Kobayashi, T.Fujimoto and J.S.Epstein, Finite element analyses of near-tip deformation in inhomogeneous elastic-plastic fracture specimens, *Int. J. Pres. Ves. & Piping,* Vol.63, pp.277-291, 1995
3) H.Homma, Y.Kanto, T.Kubo, and Y.Tanaka, Crack growth resistance in bi-metallic weldment, *Int. J. Pres. Ves. & Piping*, Vol.63, pp.225-236, 1995
4) Y.Arai, M.Kikuchi, T. Watanabe, and M. Nakagaki, Residual stress due to welding and its effect on the assessment of cracks near the weld interface, *Int. J. Pres. Ves. & Piping,* Vol.63, pp.237-248, 1995
5) M.C. Burstow and R.A.Ainsworth, Comparison of analytical, numerical and experimental solutions to problems of deeply cracked welded joints in bending, Fatigue *Fract. Engng. Mater. Struct.* Vol.18, No.2, pp.221-234, 1995
6) J.Spurrier, P.Hancock and J.P.Chubb, An assessment of weld mis-matching, *Engineering Fracture Mechanics*, Vol.53, pp.581-592, 1996
7) I.Milne, R.A.Ainsworth, A.R.Dowling, and A.T.Stewart, Assessment of integrity of structures containing defects, *Int. J . Pres. Ves. & Piping,* Vol.32, pp.3-104, 1988
8) I.Milne, R.A.Ainsworth, A.R.Dowling, and A.T.Stewart, Background to and validation of CEGB report R/H/R6--revision 3, *Int. J. Pres. Ves. & Piping,* Vol.32, pp.3-104, 1988
9) R.A.Ainsworth, Failure assessment diagrams for use in R6 assessments for austenitic components, *Int. J. Pres. Ves. & Piping*, Vol.65, pp.303-309, 1996
10) Y.W.Shi, J.X.Zhang, and X.P.Zhang, An elastic-plastic fracture analysis approach and radiation embrittlement monitoring technique by means of small samples for nuclear pressure vessel, Final Report for appraisal, No.75-19-03-05, Xi'an Jiao-tong University, Xi'an, 1990.
11) H.Yoshinari, On the methods for fracture strength assessment, *Journal of the Japan Welding Society,* Vol.64, pp.422-431, 1995
12) ABAQUS/Standard User's Manual, Version 5.5, Hibbitt, Karlsson & Sorensen, Inc. logo, USA, 1995.
13) W.Tang and Y.W.Shi, Influence of strength matching and crack depth on fracture toughness of welded joints, *Engineering Fracture Mechanics,* Vol.51, pp.649-659, 1995
14) J.Xie and Y.W.Shi, Effect of yield stress and specimen size on the position of fracture toughness peak(FTP) in $J_i - a/W$ curves, *Engineering Fracture Mechanics,* Vol.33, pp.907-912, 1989